Fluid avalanches

Christophe Ancey

March 2014

Outline

- Context: the dam-break problem
- Laboratory insight: flow visualization
  - Newtonian flow
  - Viscoplastic material
  - Concentrated particle suspension
- Summary and references

The dam-break problem

In engineering, dam break: sudden release of water

Teton dambreak (Idaho, 1976)

Scientific issues

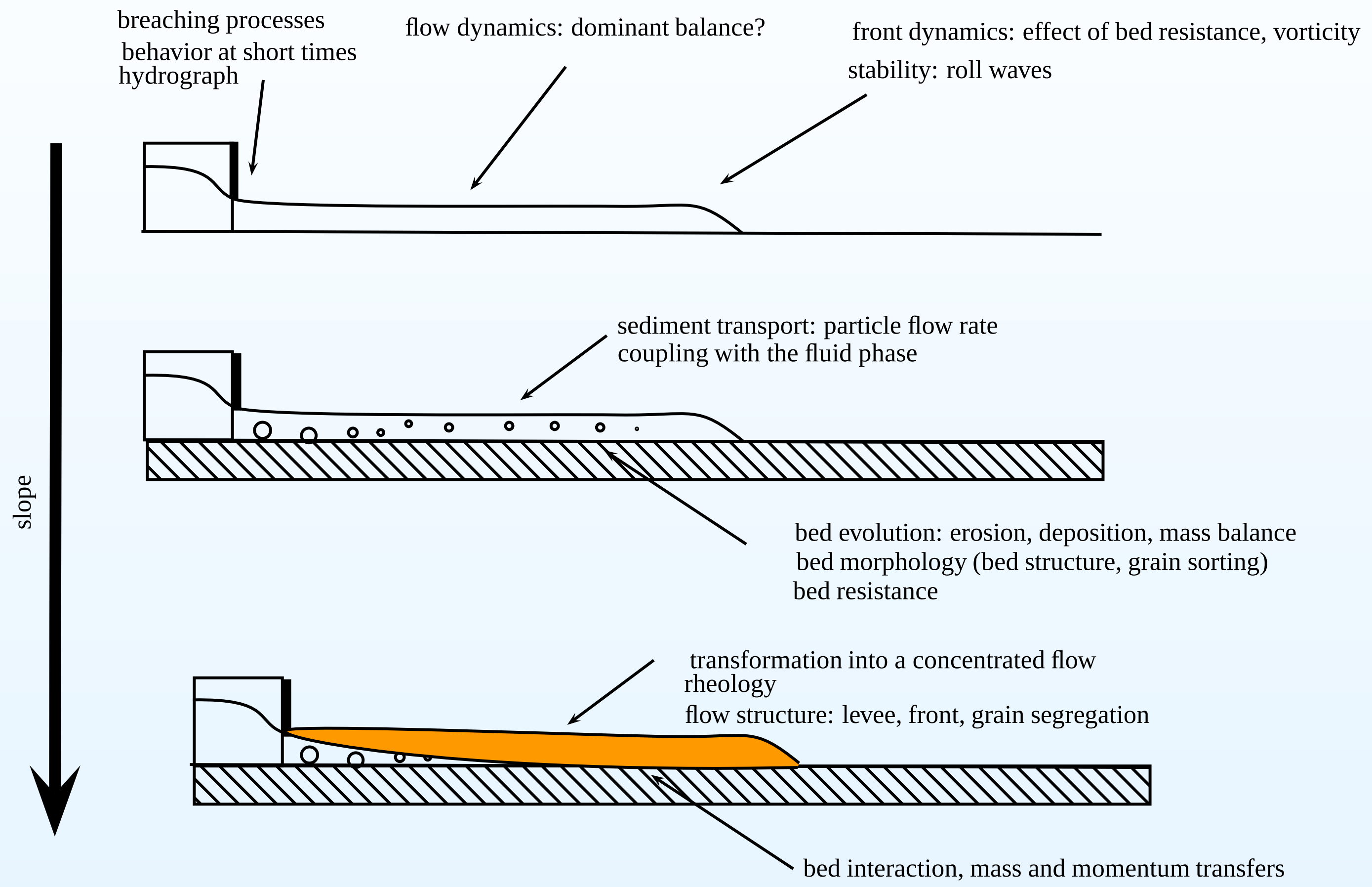

Induced sediment transport

Taum Sauk dam break (Missouri, Dec. 2005) intense erosion of the bed (down to the bed rock) and sediment transport

Related phenomena

Outburst flood: Lake Nostetuko (British Columbia, Canada) July 1983

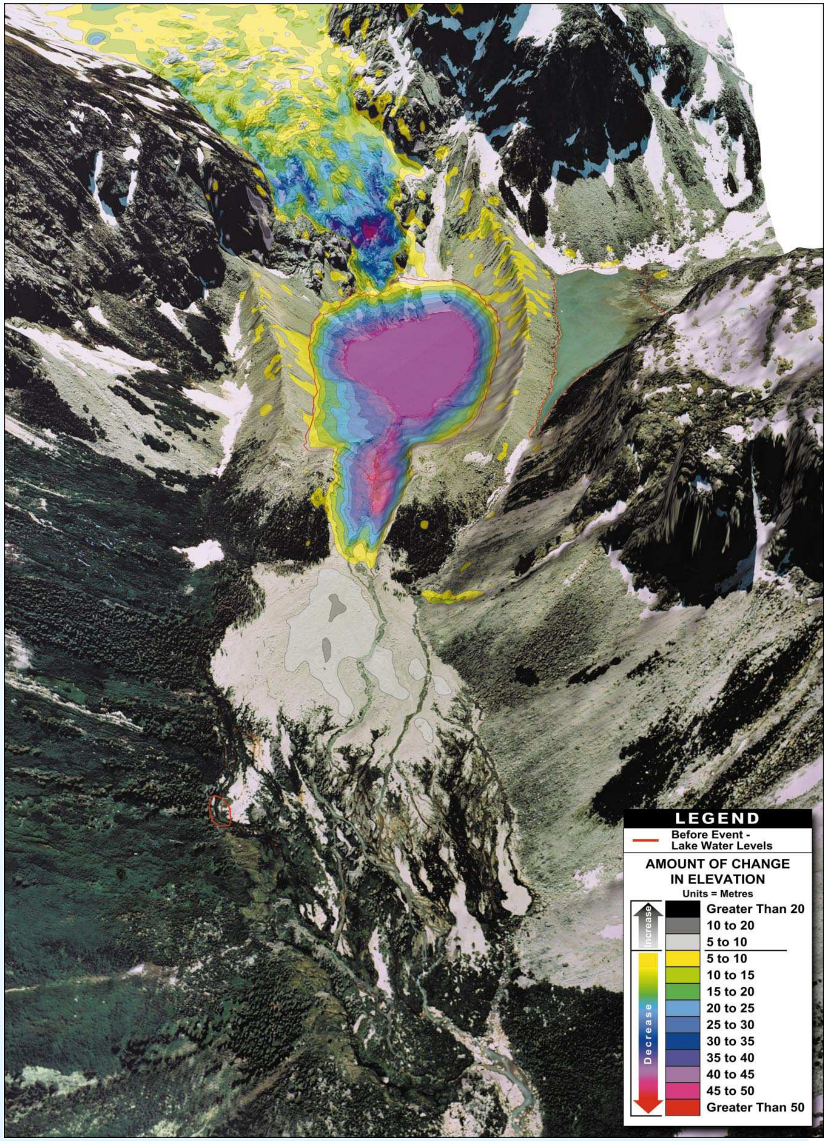

Muddy debris flow

Glide avalanches

Laboratory avalanches

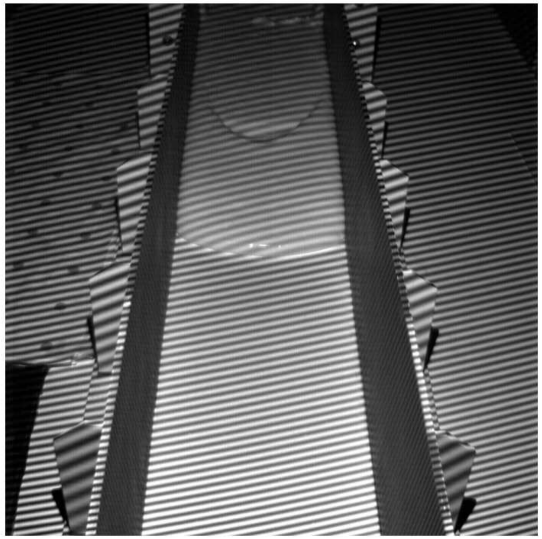

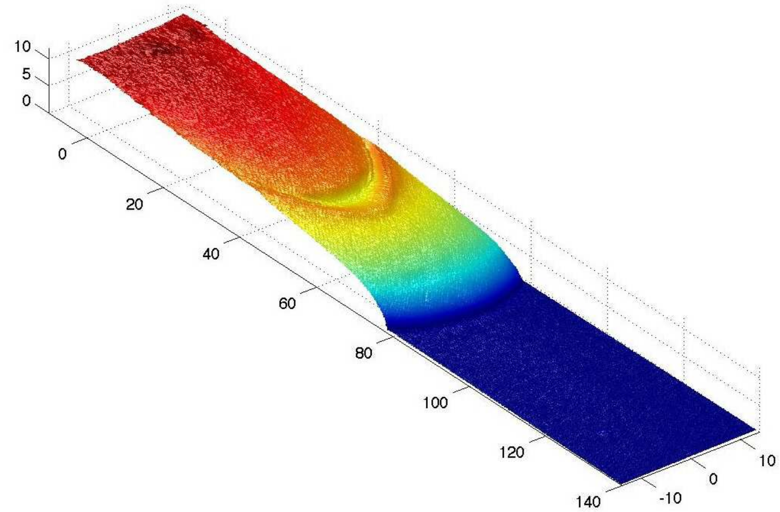

ÉCOLE POLYTECHNIQUE
FÉDÉRALE DE LAUSANNE

The dam-break problem

Release of a fixed volume of fluid

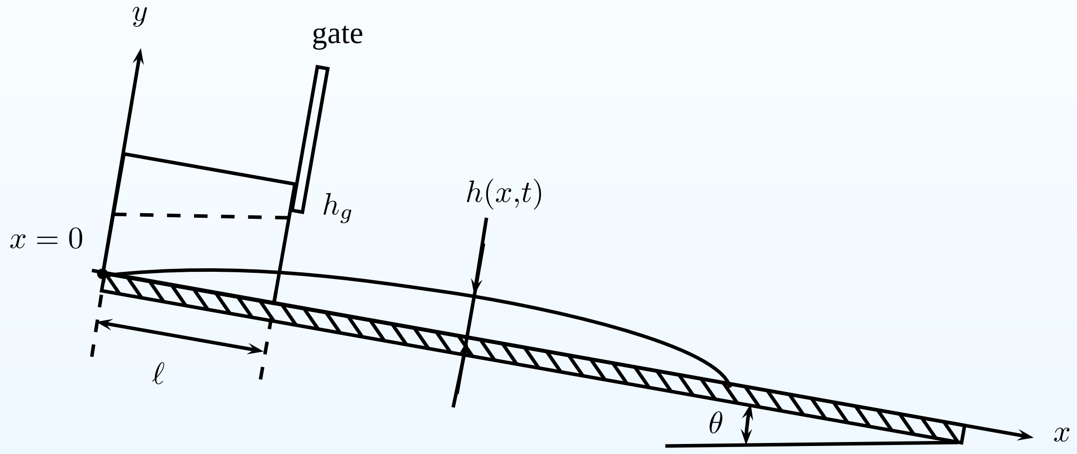

Questions:

- Front position over time $x_f(t)$?
- Flow depth profile $h(x,t)$?
- Velocity profile within the flow (far from the sidewall) ?
- Further questions: stability, slip, influence of surface tension, etc.

Navier-Stokes equations

Dimensionless form

$$
\begin{aligned}
\frac{\partial u}{\partial x} + \frac{\partial v}{\partial y} &= 0, \\
\epsilon \mathrm{Re} \frac{\mathrm{d}u}{\mathrm{d}t} &= \phi \cos\theta \left(\tan\theta - \epsilon \frac{\partial p}{\partial x} \right) + \epsilon^2 \frac{\partial^2 u}{\partial x^2} + \frac{\partial^2 u}{\partial y^2}, \\
\epsilon^2 \mathrm{Re} \frac{\mathrm{d}v}{\mathrm{d}t} &= -\phi \cos\theta \left(1 + \frac{\partial p}{\partial y} \right) + \epsilon^3 \frac{\partial^2 v}{\partial x^2} + \epsilon \frac{\partial^2 v}{\partial y^2},
\end{aligned}
$$

with $\phi = \rho g H_*^2/(\mu U_*)$ a dimensionless group and $\epsilon = H_*/L_* \ll 1$ the aspect ratio.

$Ca = \mu U_*/\gamma \gg 1$ and $Re = \rho U_* H_*/\mu \ll 1$: capillary and Reynolds numbers.

L_* and H_* selected so that $L_* H_* = \tilde{V}$, viz, $L_* = \sqrt{\tilde{V}/\epsilon}$ and $H_* = \sqrt{\epsilon \tilde{V}}$

Flow regimes

Dominant balance:

- *Diffusive regime*. Balance between the pressure and shear stress gradients : $U_* = \rho g H_*^3/(3\mu L_*)$ and $\phi = 3/\epsilon$
- *Advection diffusion regime.* Balance between the body force and shear stress gradient + pressure gradient within the leading edge: $\epsilon = \tan\theta$, $U_* = \rho g H_*^2 \sin\theta/(3\mu)$, and $\phi = 3/\sin\theta$
- *Steep slope regime*. Increasing role of the body force: $\epsilon = \tan^2\theta$, $U_* = \rho g H_*^2 \sin\theta/(3\mu)$, and $\phi = 3/\sin\theta$

Diffusive regime

Diffusive regime observed for $Ca \to \infty$, $Re = O(1)$, and $\theta \ll 1$.
Dimensionless governing equation for $\theta > 0$

$$\frac{\partial h}{\partial t} + \frac{\partial h^3}{\partial x} = \frac{\partial}{\partial x}\left(h^3 \frac{\partial h}{\partial x}\right).$$

Dimensionless governing equation for $\theta = 0$

$$\frac{\partial h}{\partial t} = \frac{\partial}{\partial x}\left(h^3 \frac{\partial h}{\partial x}\right).$$

No analytical solution (available), but asymptotic solutions at short or long times t with the following change of variable

$$h(x,t) = t^{-n} H(\xi, t)$$

- short-time solution: $n = 1/5$ (Nakaya, 1974 ; Huppert, 1982) ;
- long-time solution: $n = 1/3$ (Huppert, 1982 ; Lister, 1982).

Diffusive regime at $t \ll 1$

Huppert's (or Barrenblatt-Pattle's) solution

$$h(x,t) = t^{-1/5}\left(\frac{3}{10}(\xi_f^2 - \xi^2)\right)^{1/3} \text{ avec } \xi_f = V_0^{3/5}\left(\frac{\sqrt[3]{\frac{3}{10}}\sqrt{\pi}\,\Gamma\left(\frac{1}{3}\right)}{5\Gamma\left(\frac{5}{6}\right)}\right)^{-3/}$$

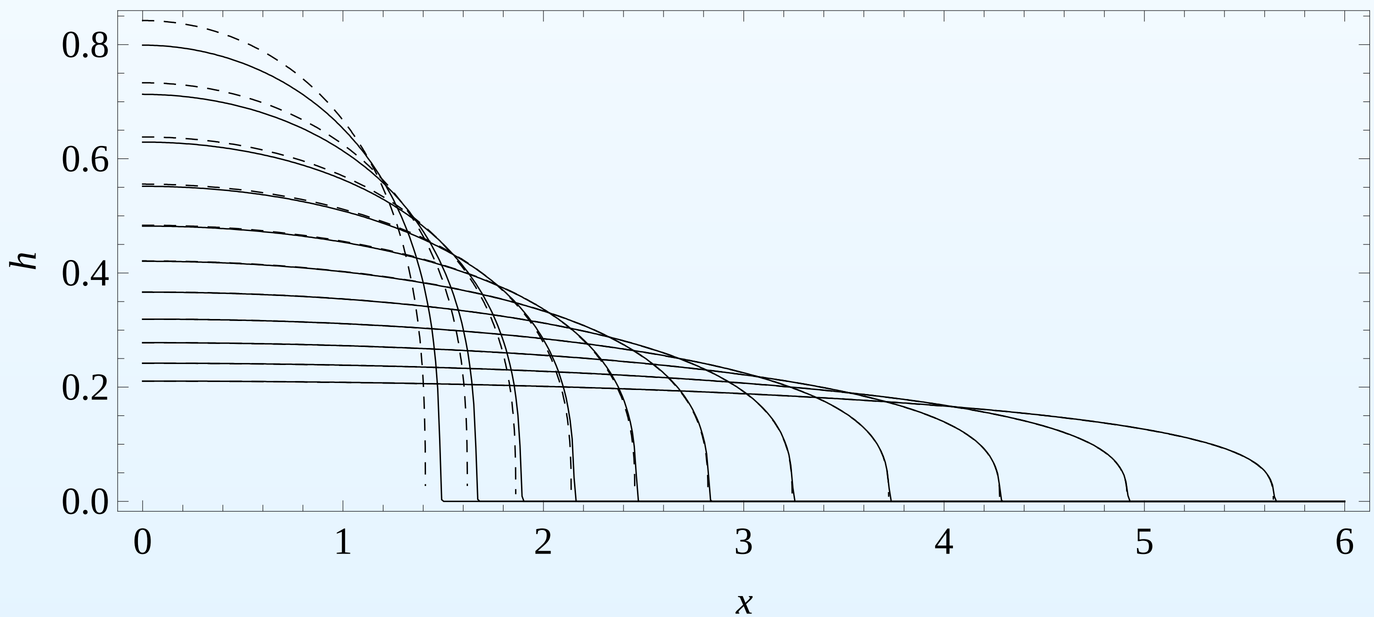

Comparison between the numerical solution and Huppert's self-similar solution at $t = 1$, 2, 4, 8, 16, 32, 64, 128, 256, 512, and 1024

Diffusive regime at $t \gg 1$

Huppert's solution (+ higher-order terms Ancey, JFM 2009)

$$h(x,t) = t^{-1/3}\left(\sqrt{\frac{1}{3}\frac{x}{t^{1/3}}} + K_0\left((\xi_f - xt^{1/3})t^{2/3}\right) - \sqrt{\frac{\xi_f}{3}}\right).$$

with the position of the front given by

$$x_f = \xi_f t^{1/3} + \left(\log 2 - \frac{1}{2}\right)\sqrt{\frac{\xi_f}{3}}t^{-1/3},$$

with

$$\xi_f = \left(\frac{3\sqrt{3}}{2}V\right)^{2/3}$$

This solution requires a boundary-layer treatment at the front as the diffusive effects (pressure gradient) prevail over the advection term.

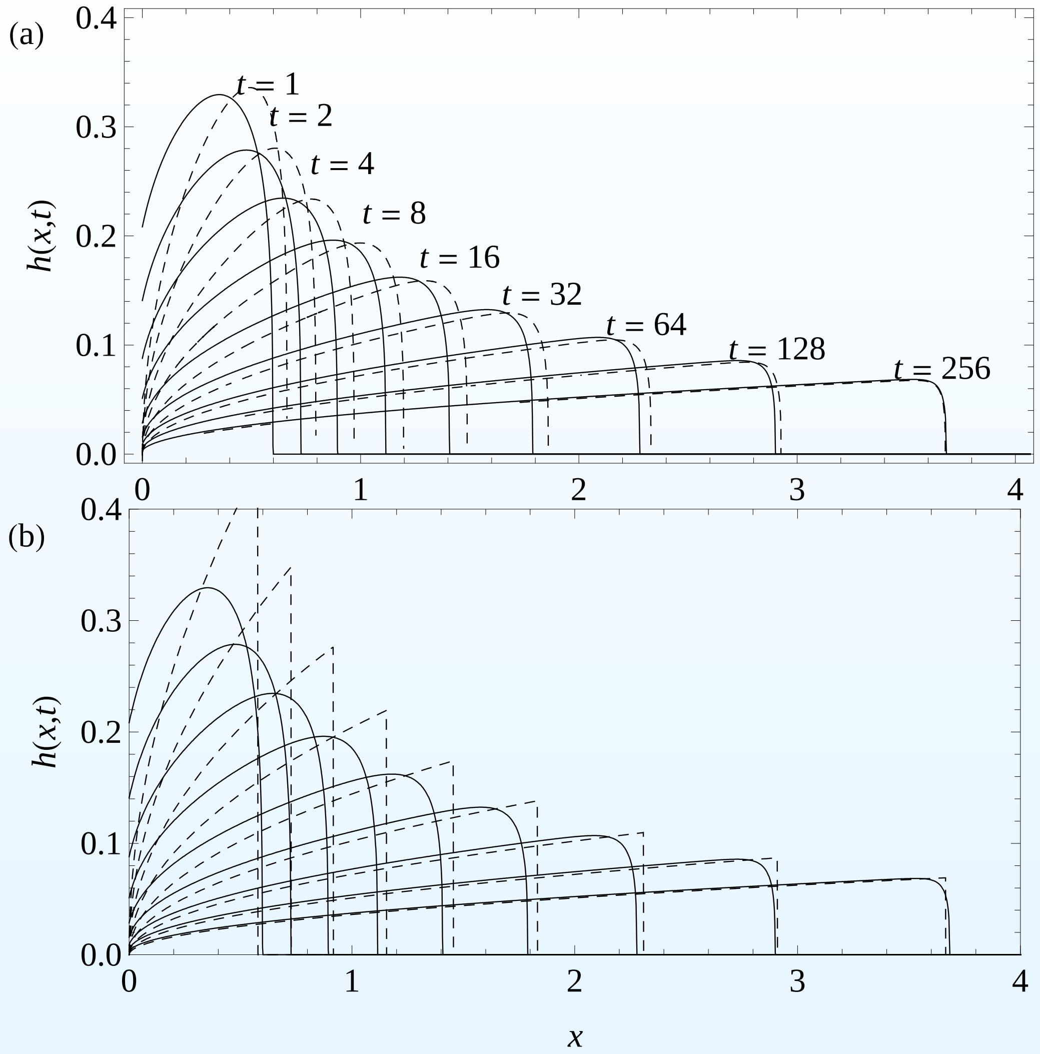

Comparison of flow depth profiles: numerical solution (solid line) and asymptotic solution (dashed line), with diffusion included (a) or not (b), for slope $\theta = 6^{\circ}$, at times $t = 1$, 2, 4, 8, 16, 32, 64, 128, and 256.

Comparison with experiments

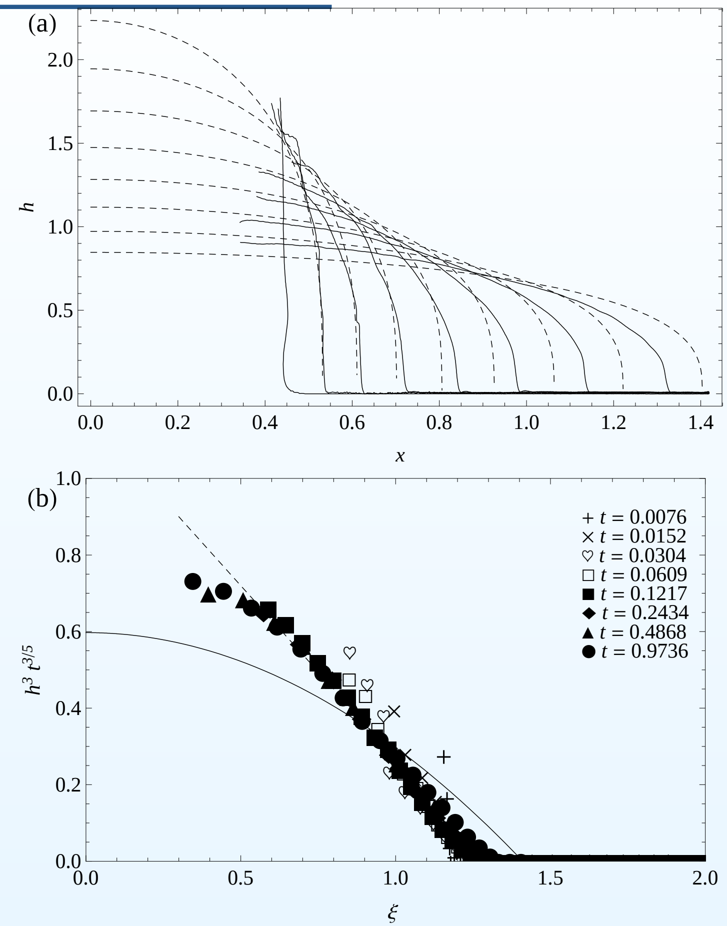

Comparison of flow depth profiles for $\theta = 0°$. For (b), we show the self-similar solution and the experimental trend $(h/t^{-1/5})^3 = \frac{9}{10}(1.3 - \xi)$. Fluid: glucose ($\mu = 345$ Pa s)

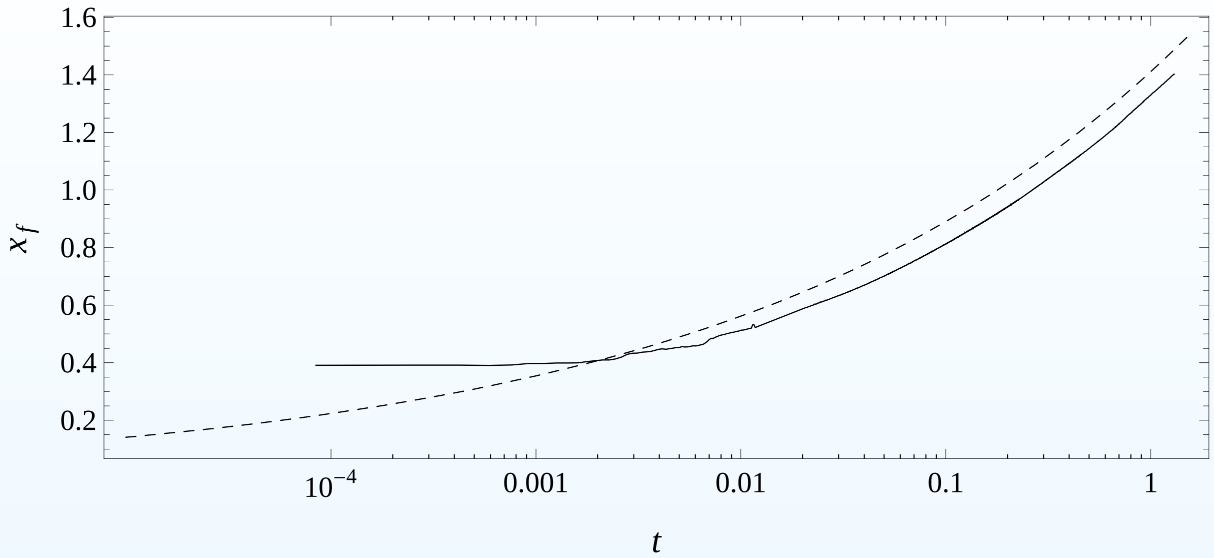

Front position over time: experimental data (solid line) and theory (dashed line)

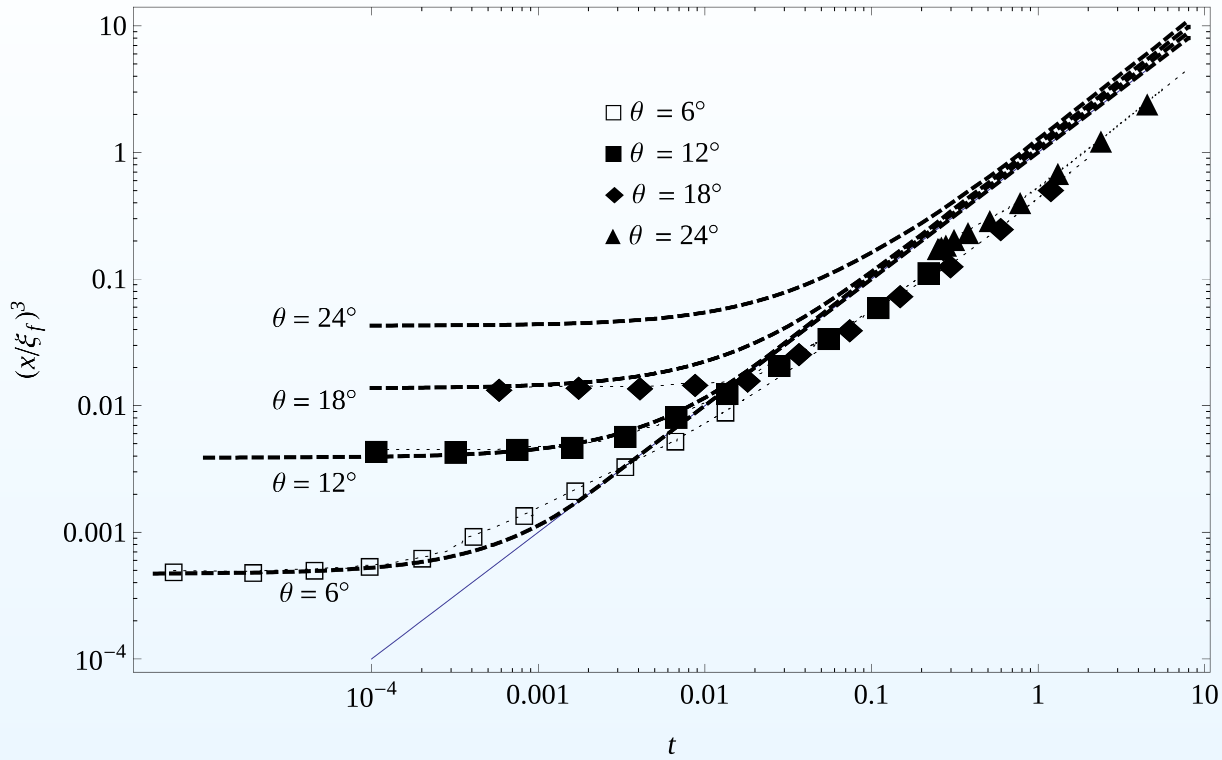

Front position over time for slopes ranging from $6°$ to $24°$

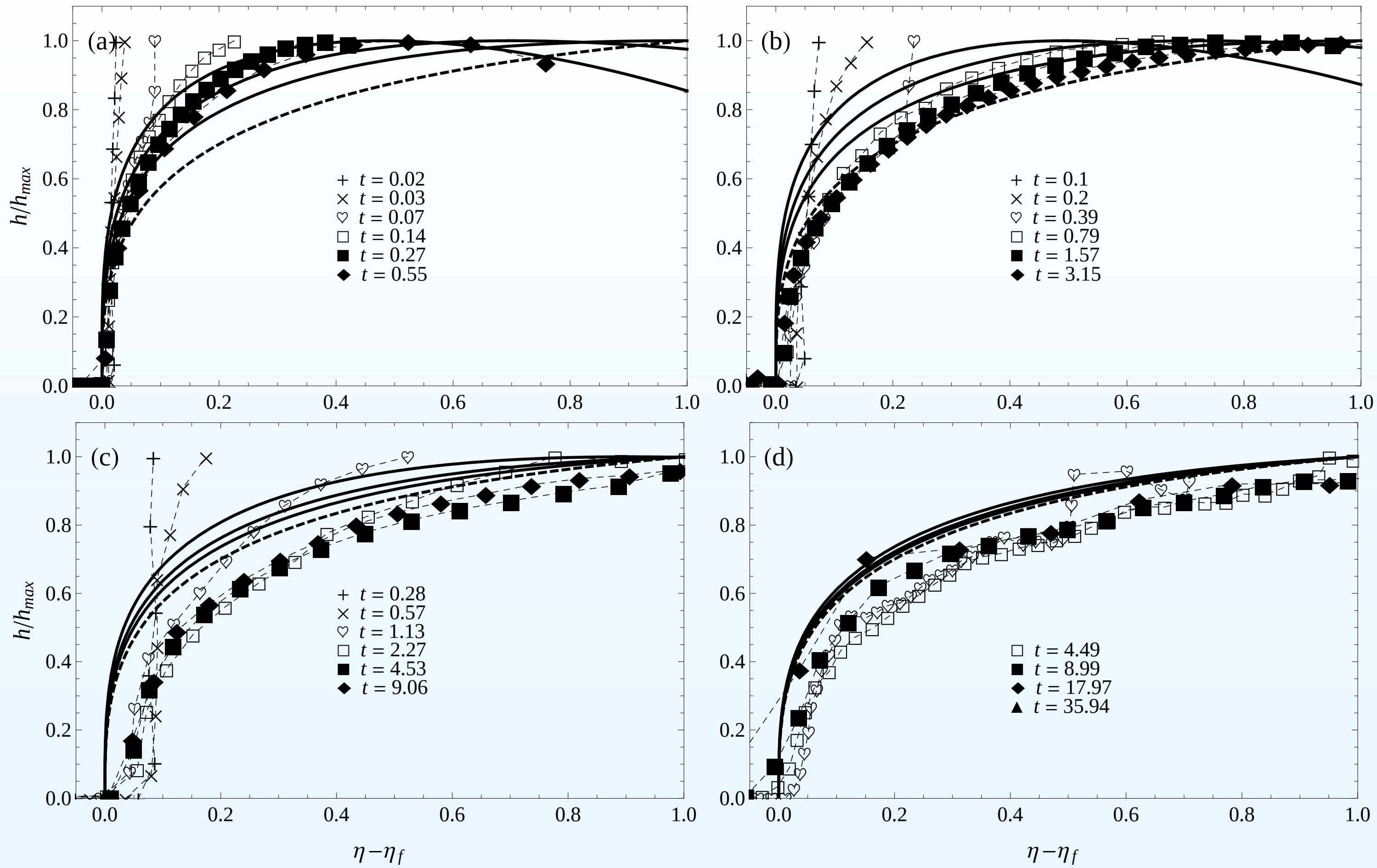

Flow depth profiles for slopes ranging from 6° to 24° and different slopes

ÉCOLE POLYTECHNIQUE
FÉDÉRALE DE LAUSANNE

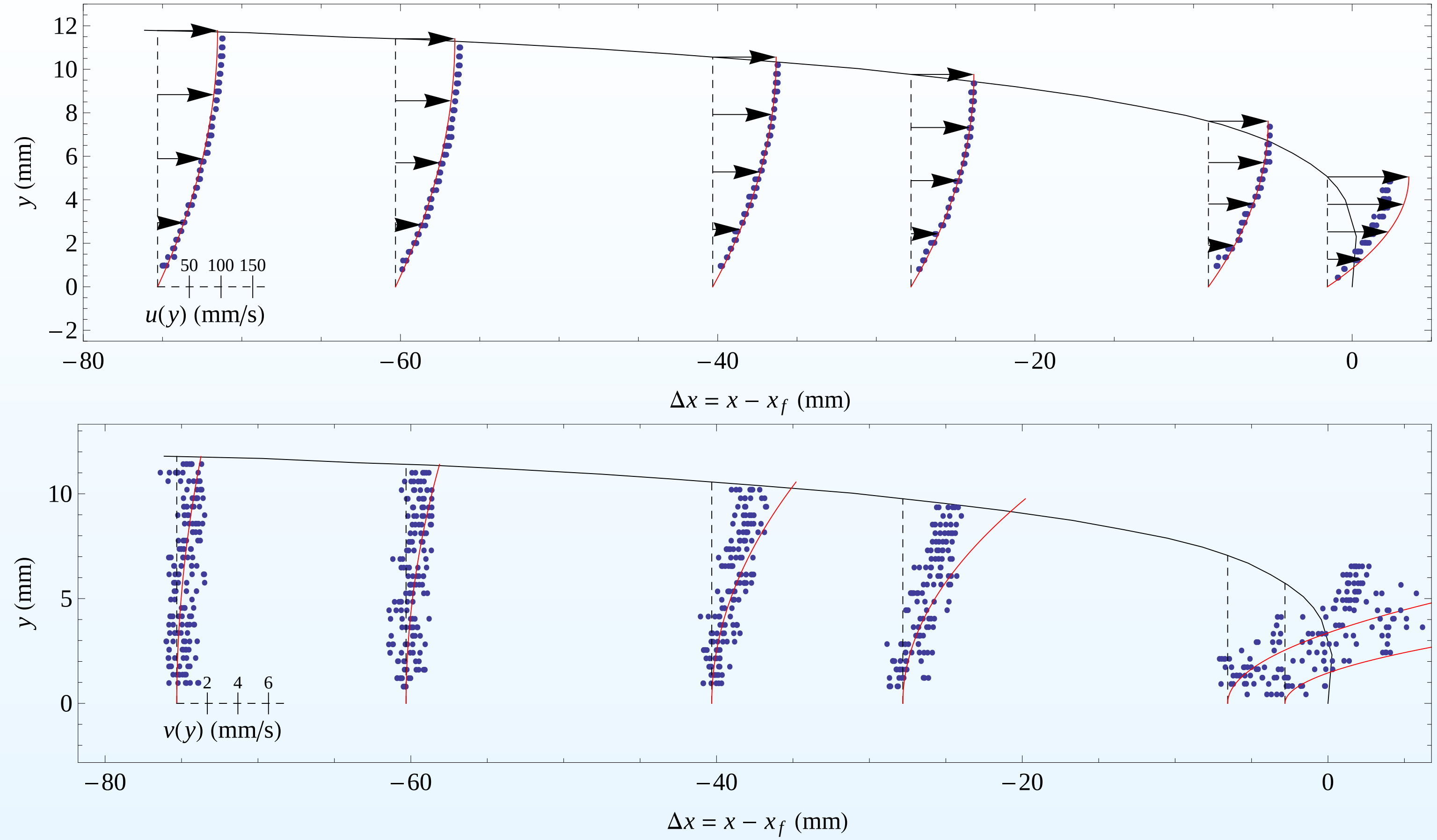

Velocity profiles (u and v) in glycerol ($\mu = 1.11$ Pa s) for a 6° slope

ÉCOLE POLYTECHNIQUE
FÉDÉRALE DE LAUSANNE

Viscoplastic material

Simple shear constitutive law

$$\mu\dot{\gamma}^n = \begin{cases} \tau - \tau_c & \text{for } \tau > \tau_c, \\ 0 & \text{for } \tau \leq \tau_c, \end{cases}$$

Velocity profile for $y \leq Y_0$ or $y > Y_0$ (Liu & Mei, 1990)

$$u(x,y,t) = \begin{cases} \dfrac{n}{n+1} K \left(Y_0^{1+1/n} - (Y_0 - y)^{1+1/n} \right) \left(1 - \cot\theta \dfrac{\partial h}{\partial x} \right) \\ \dfrac{n}{n+1} K \left(1 - \cot\theta \dfrac{\partial h}{\partial x} \right) Y_0^{1+1/n}, \end{cases}$$

where $Y_0 = \max(0, h - \tau_c/(\rho g \cos\theta(\tan\theta - \partial_x h)))$ denotes the position of the yield surface and $K = \rho g \sin\theta/\mu$.

Comparison with experiments

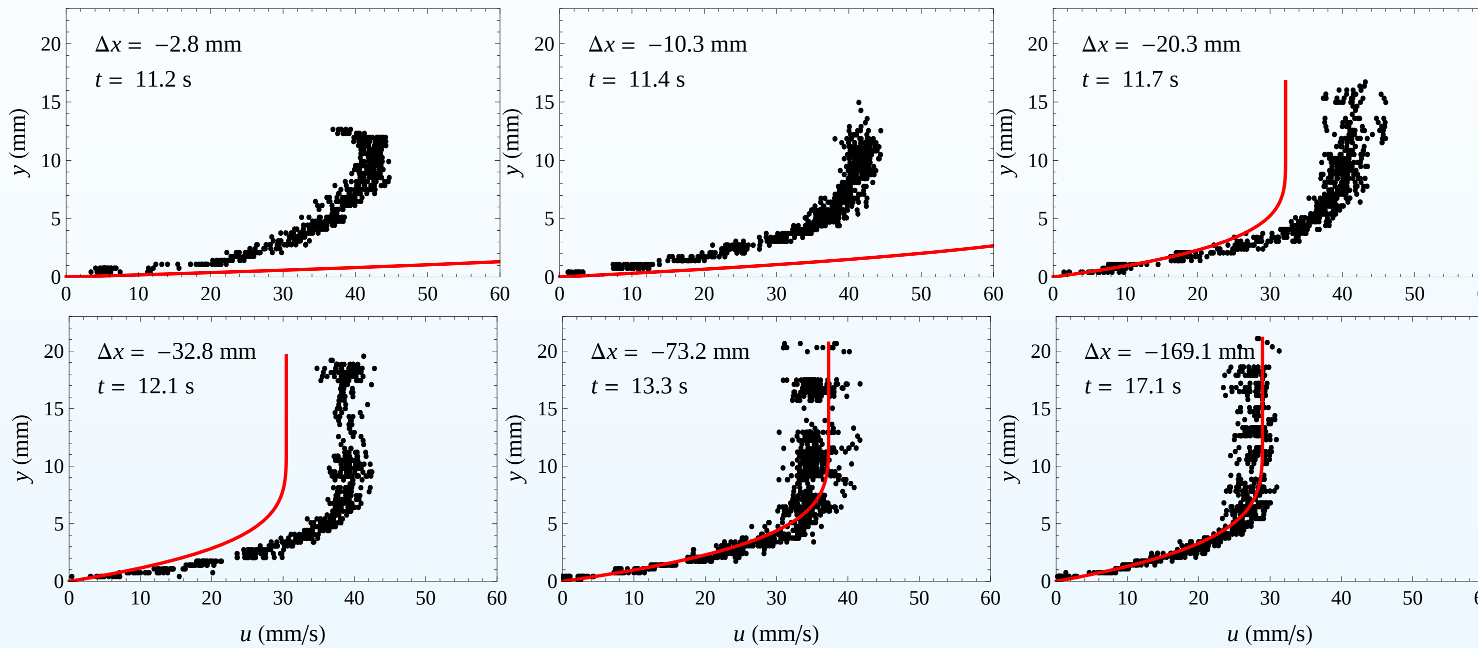

Comparison of the velocity profiles for $\theta = 25°$ at different distances Δx to the front. Fluid: Carbopol ultrez 10 ($\mu = 26$ Pa s^n, $n = 0.33$, $\tau_c = 33$ Pa)

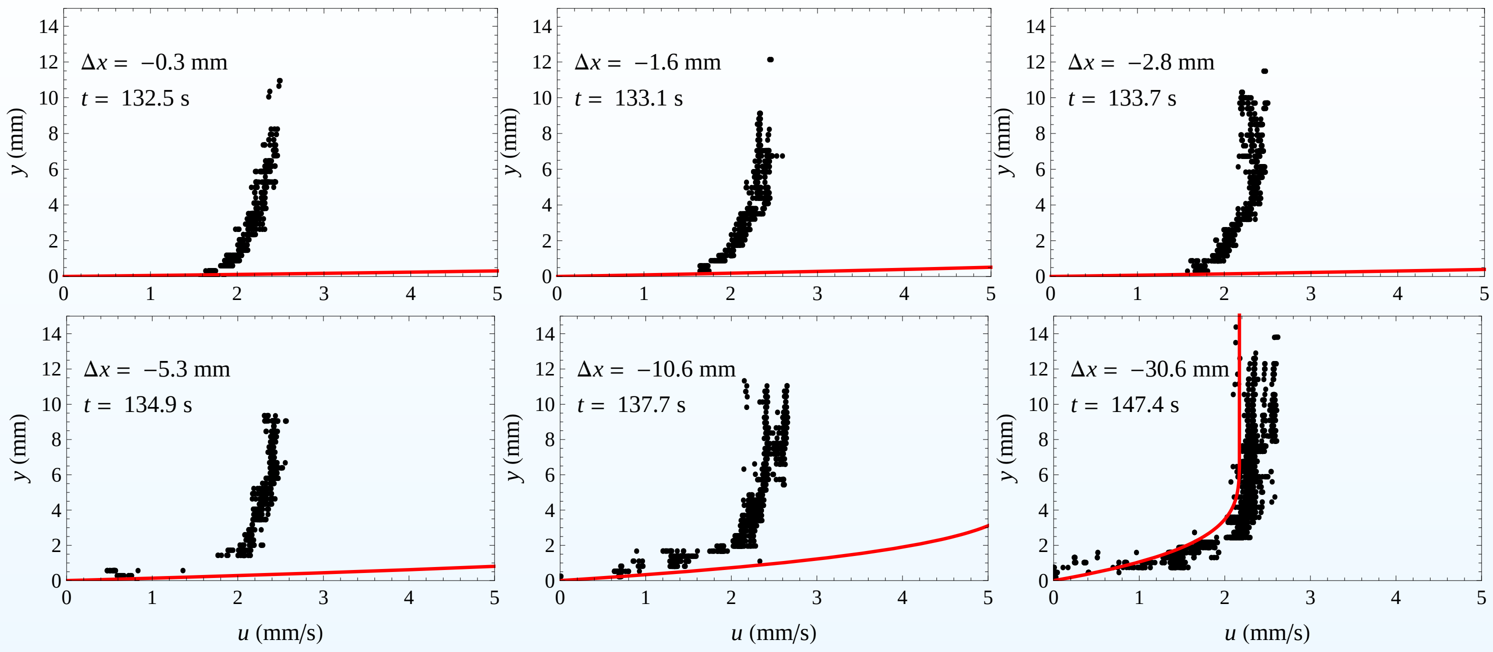

Comparison of the velocity profiles for $\theta = 15^\circ$ at different distances to the front. Fluid: Carbopol ultrez 10 ($\mu = 26$ Pa s^n, $n = 0.33$, $\tau_c = 33$ Pa)

Flow models

Dimensionless depth-averaged equations (e.g. Craster & Mater, 2009)

$$\frac{\partial h}{\partial t} + \frac{\partial h\bar{u}}{\partial x} = 0,$$

$$\epsilon Re \left(\frac{\partial h\bar{u}}{\partial t} + \beta \frac{\partial h\bar{u}^2}{\partial x} \right) + \epsilon \cot\theta h \frac{\partial h}{\partial x} = h - \tau_b + \frac{\epsilon^3}{Ca} h \frac{\partial^3 h}{\partial x^3}.$$

Several simplifications developed:

- kinematic wave model (Huang & Garcia, 1994): balance between the driving and ‘viscous’ forces;
- diffusive wave model: balance between the driving and ‘viscous’ forces + pressure gradient;
- Saint-Venant model: in the limit of $Ca \to \infty$ and $\epsilon \ll 1$, with a closure equation for τ_b.

Kinematic wave model

A simple nonlinear advection equation (hyperbolic)

$$\frac{\partial h}{\partial t} + \frac{\partial h\bar{u}}{\partial x} = 0$$

Analytical solutions (using the method of characteristics) in an implicit form. For a 25° slope

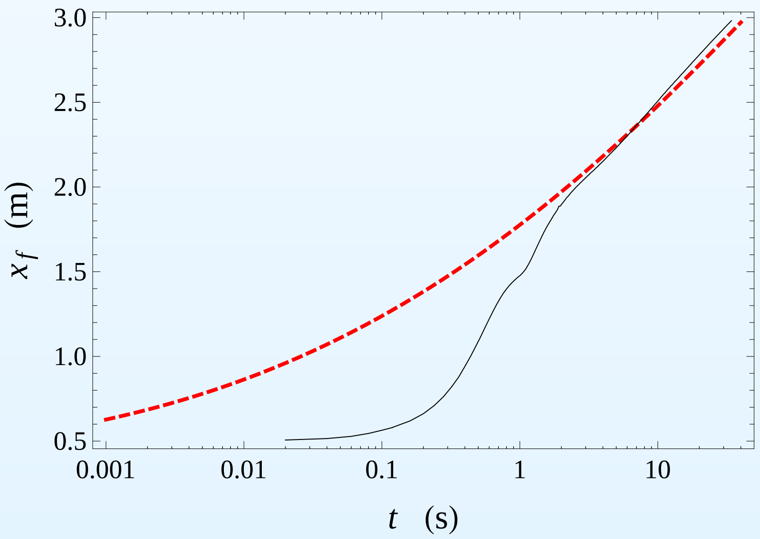

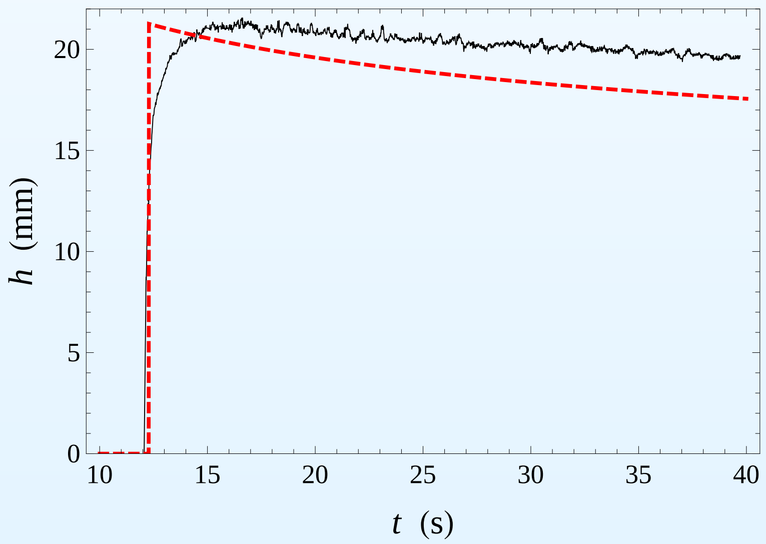

For a 15° slope

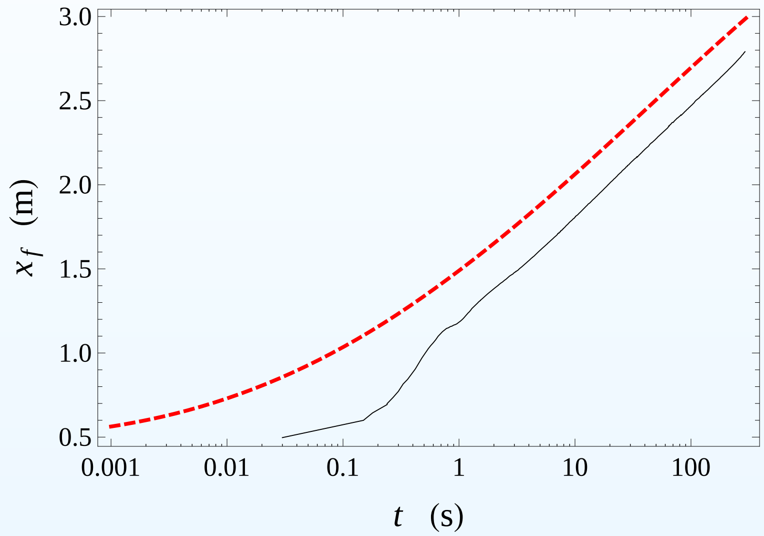

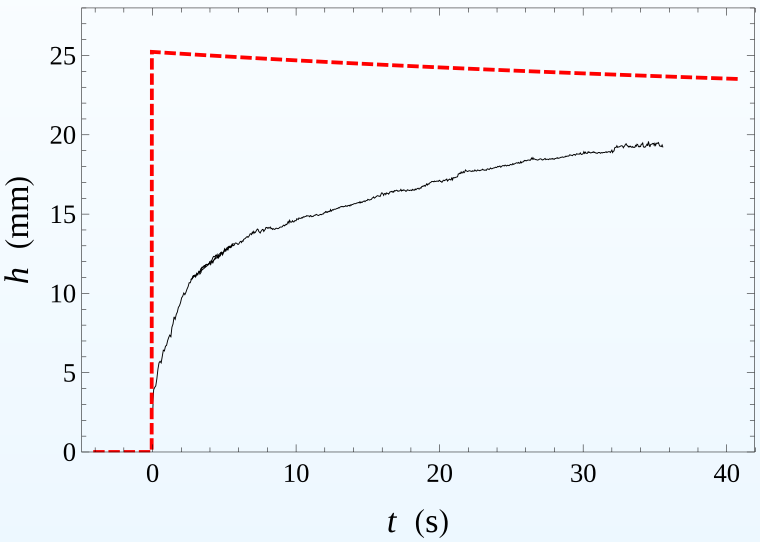

Diffusive wave equation

A nonlinear advection-diffusion equation (parabolic)

$$\frac{\partial h}{\partial t} + nK\frac{\partial}{\partial x}\left[\left(\tan\theta - \frac{\partial h}{\partial x}\right)^{1/n}\frac{h(1+n)+nh_c}{(n+1)(2n+1)}Y_0^{1+1/n}\right] = 0$$

No analytical solution.

For a 25° slope

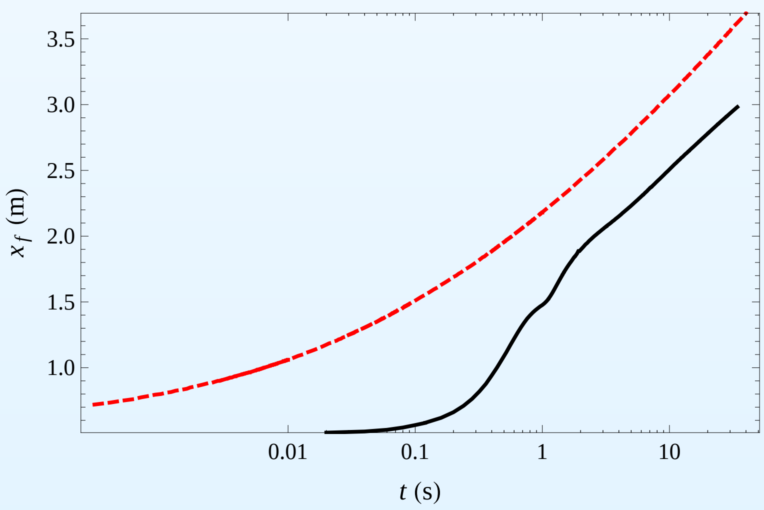

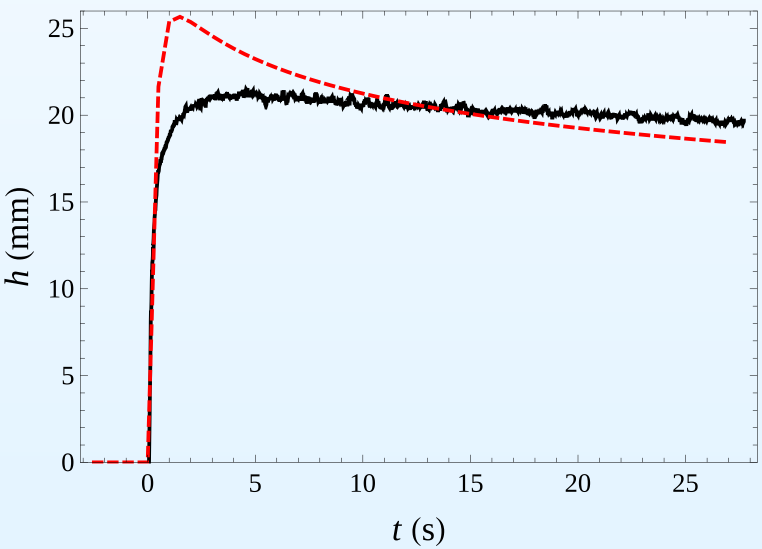

For a 15° slope

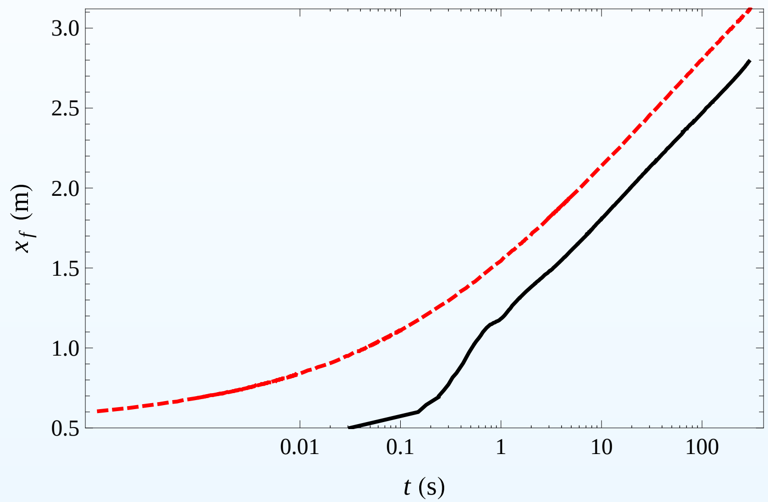

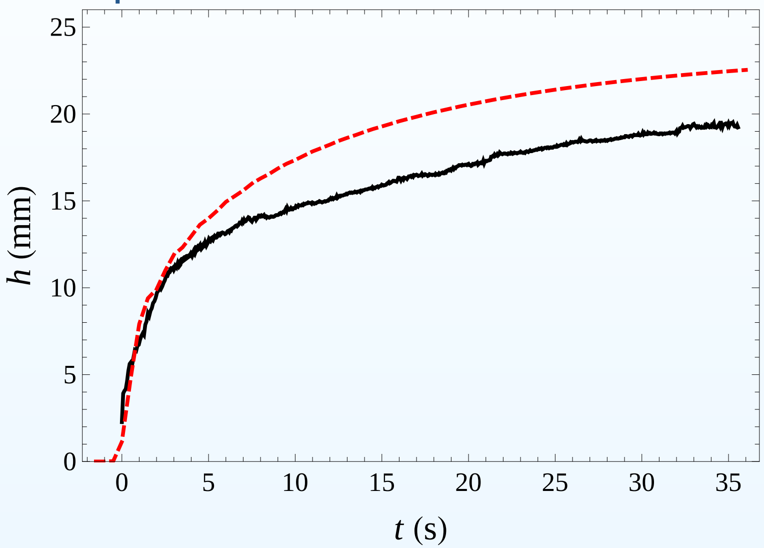

Saint-Venant model

Hyperbolic partial differential equations

$$\begin{aligned} \frac{\partial h}{\partial t} + \frac{\partial h\bar{u}}{\partial x} &= 0, \\ \frac{\partial h\bar{u}}{\partial t} + \frac{\partial h\bar{u}^2}{\partial x} + gh\cos\theta\frac{\partial h}{\partial x} &= gh\sin\theta - \frac{\tau_b}{\rho}, \end{aligned}$$

Coussot's closure equation:

$$\tau_b = \tau_c\left(1 + 1.93G^{3/10}\right) \text{ with } G = \left(\frac{\mu}{\tau_c}\right)^3\frac{\bar{u}}{h}$$

ÉCOLE POLYTECHNIQUE
FÉDÉRALE DE LAUSANNE

For a 25° slope

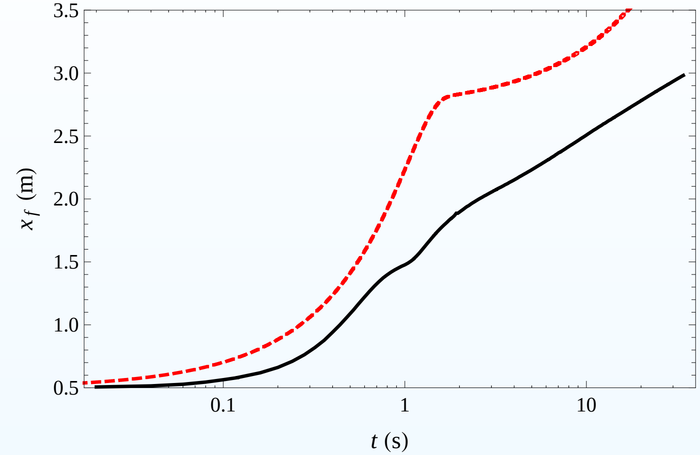

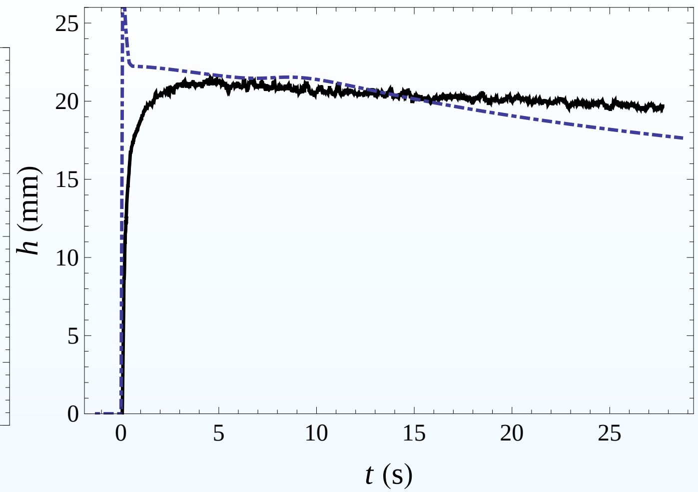

For a 15° slope

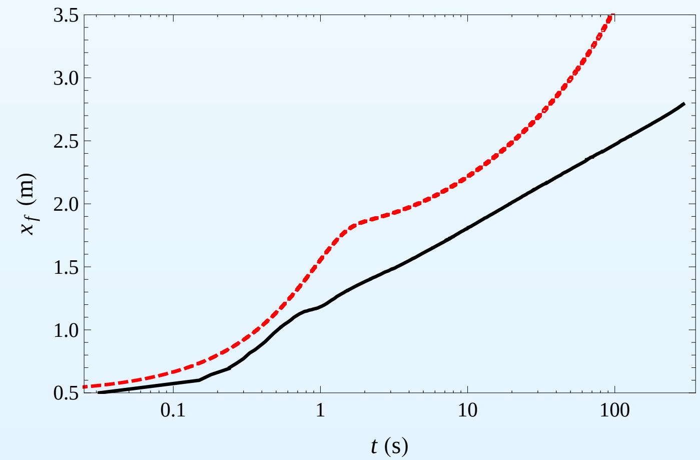

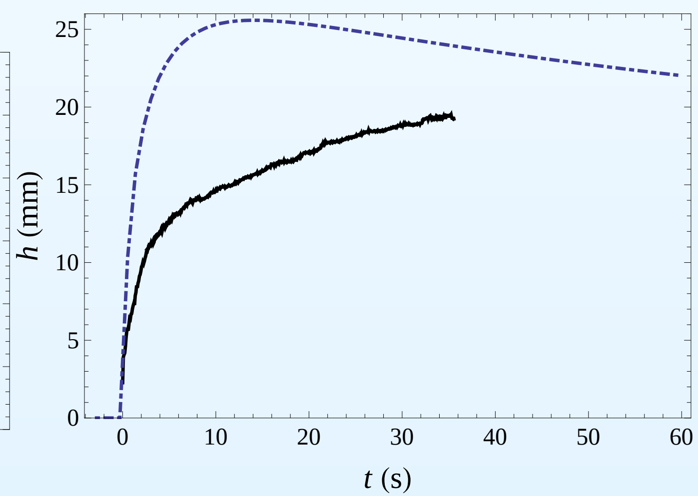

ÉCOLE POLYTECHNIQUE
FÉDÉRALE DE LAUSANNE

Scientific issues

A density-matched suspension of particles within a Newtonian carrier fluid is assumed to be quasi-Newtonian:

- effective viscosity given by empirical laws, e.g.,

$$\eta(\phi) = \frac{\mu(\phi)}{\mu_f} = \left(1 - \frac{\phi}{\phi_m}\right)^{-\beta}$$

  ϕ_m the maximum concentration and β a constant : $\beta = \frac{5}{2}\phi_m$ or $\beta = 2$ (Krieger & Dougherty 1959)

- occurrence of normal stress effects (Zarraga *et al.* JOR, 2001 ; Boyer et al. JFM 2001 ; Couturier *et al.* JFM 2011)

Problem: particle migration occurs even for $\Delta\rho = 0$ (effect exacerbated when sedimentation or creaming occurs, depending on $\Delta\rho > 0$ or $\Delta\rho < 0$), so this results in a nonhomogeneous spatial distribution of the particles, thus viscosity.

Particle migration

Migration: stratification of particles as a result of shear. Two approaches:

- Phenomenological model developed by Leighton & Acrivos (JFM 1987)

$$\boldsymbol{j} \propto -\phi^2 \nabla \dot{\gamma} \text{ avec } \boldsymbol{j} = \phi(\boldsymbol{u}^p - \boldsymbol{u})$$

  the particle flux relative to the bulk velocity

- Microstructural approach by Nott & Brady (JFM 1994) and Morris & Boulay (JOR 1999)

$$\boldsymbol{j} \propto -\nabla \cdot \boldsymbol{\Sigma}^p$$

  The theoretical underpinning is still disputed (Lhuillier PoF 2009; Nott et al. PoF 2011).

Respective merits subject of fierce debate... with no winner

Shear-induced migration

Phillips et al.'s model (PoF 1992) in a dimensionless form

$$\boldsymbol{j} = -\phi K_c \frac{\epsilon_a^2}{\epsilon} \nabla(\phi\dot{\gamma}) - K_\mu \dot{\gamma}\phi^2 \frac{\epsilon_a^2}{\epsilon} \frac{\mathrm{d}\ln\eta}{\mathrm{d}\phi} \nabla\phi,$$

Two processes at play:

- diffusion of particles resulting from the anisotropy in the probability of encounter between two particles,
- Fick-like diffusion

Nonlinear advection diffusion equation for ϕ

$$\frac{\partial\phi}{\partial t} + u\frac{\partial\phi}{\partial x} + v\frac{\partial\phi}{\partial y} = -\nabla\cdot\boldsymbol{j}.$$

Solution for steady state uniform flows

With $\beta = 2$ and $\alpha = 3/2$ (otherwise the solution is implicit), one gets the quasi-explicit solution

$$\phi = \frac{\phi_w h}{\phi_m h - (\phi_m - \phi_w) y} \quad \text{with} \quad \frac{\phi_w}{\phi_m - \phi_w} \log \frac{\phi_m}{\phi_w} = \bar{\phi}$$

By integrating the conservation of momentum

$$\dot{\gamma} = \frac{\bar{\eta}}{\eta(\phi)}(h-y),$$

we determine velocity profiles numerically. They take the form

$$u = \kappa \left(h^n - (h-y)^n \right)$$

$n = 2$ for a Newtonian fluid. Another index to characterise the deviation of the computed velocity profile from the Newtonian profile ($m = 2/3$)

$$m = \frac{\int_0^h u(y,t)\mathrm{d}y}{hu(h,t)} = \frac{\bar{u}}{u(h,t)},$$

Variation of n with the particle concentration

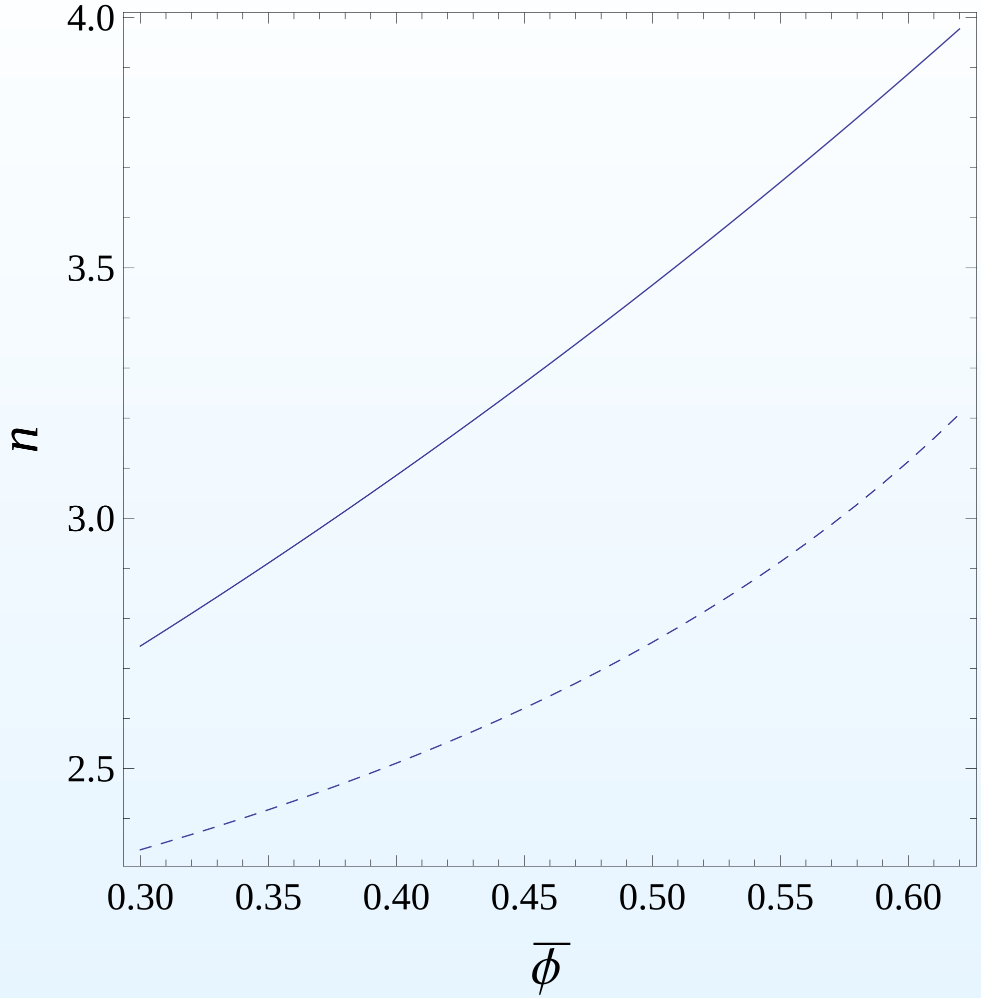

Two parameter sets: $\beta = 2$ and $\alpha = 3/2$ (solid line) ; $\beta = 2$ and $\alpha = 1.042\phi + 0.1142$ (dashed line) using the model proposed by Tetlow *et al.* (JOR 1998)

Solution for time-dependent flows

Using the assumption $\partial_x \phi = 0$

$$\frac{\partial \phi}{\partial t} = K_c \bar{\eta} \frac{\epsilon_a^2}{\epsilon} \frac{\partial}{\partial y} \left(\phi \frac{\partial}{\partial y} \left(\frac{\phi}{\eta(\phi)} (h - y) \right) + \alpha \frac{\phi^2}{\eta(\phi)} (h - y) \frac{\mathrm{d} \ln \eta}{\mathrm{d}\phi} \frac{\partial \phi}{\partial y} \right).$$

Steady state is reached at time

$$t_c \sim \frac{\epsilon}{\epsilon_a^2} = \frac{H_*^3}{a^2 L_*}$$

Numerically one gets

$$t_{ss} = 2 t_c \left(1 - \frac{\phi}{\phi_m} \right)^{-1/3}$$

ÉCOLE POLYTECHNIQUE
FÉDÉRALE DE LAUSANNE

Variation of n (and m) at short times

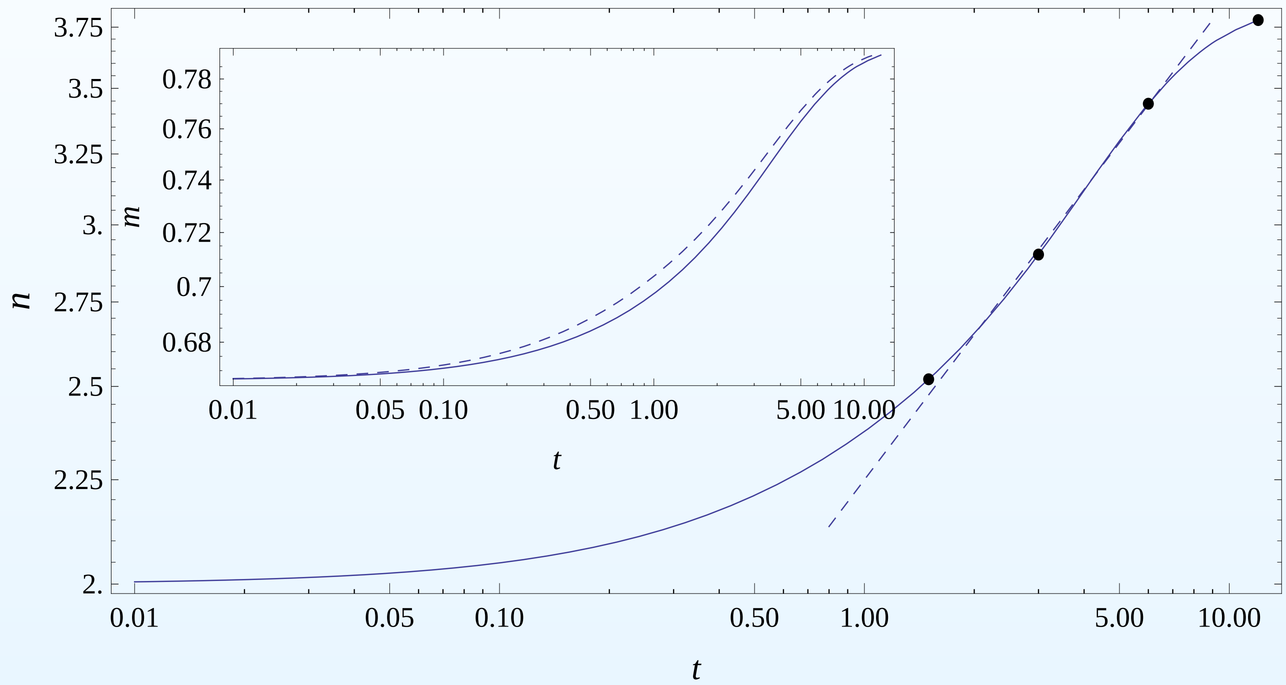

Trend $n = 2.2t^{1/4}$. Computations done for $\bar{\phi} = 52\%$, $K_c\bar{\eta}\epsilon_a^2/\epsilon = 1$, $\beta = 2$, and $\alpha = 3/2$. Computed steady state time: $t_{ss} = 3.56$.

ÉCOLE POLYTECHNIQUE
FÉDÉRALE DE LAUSANNE

Comparison with experiments

Variation of $x_f(t)$ (dimensionless)

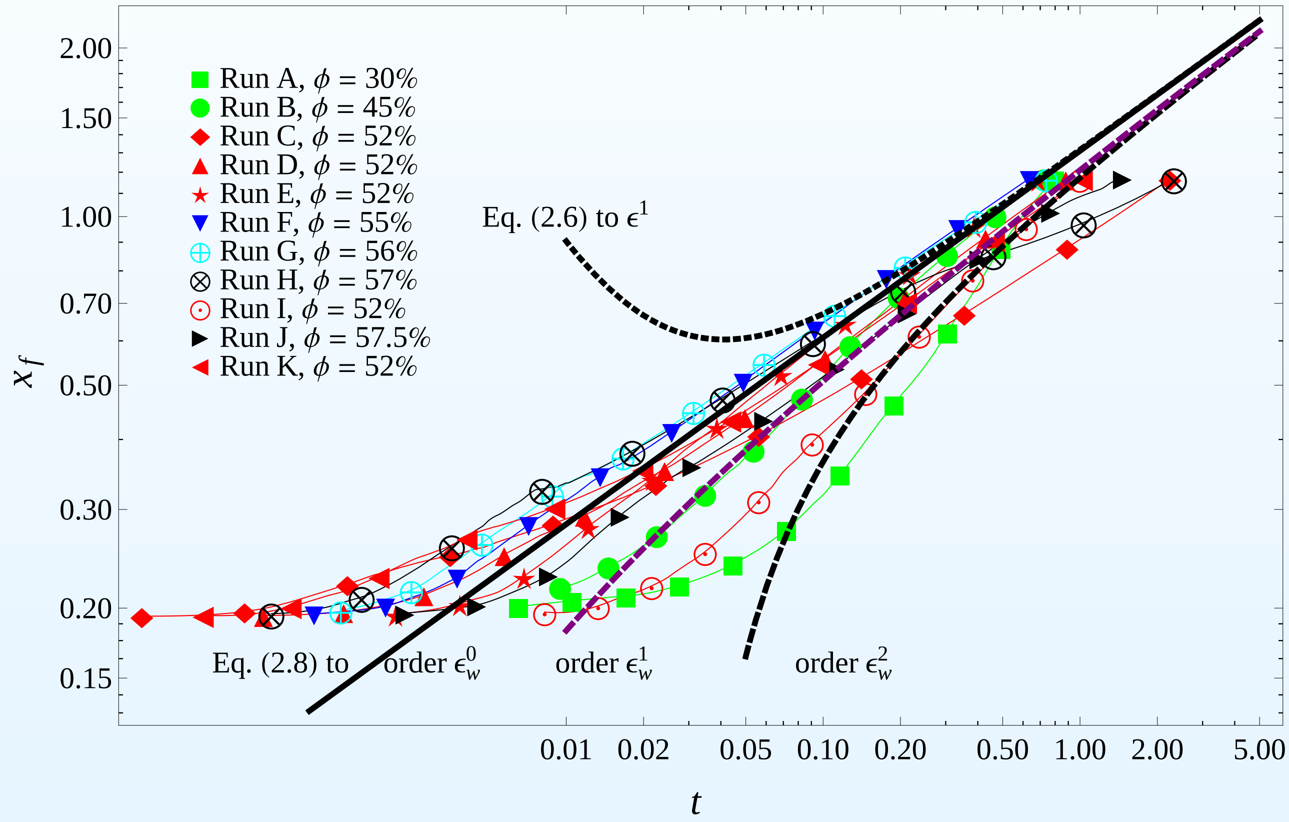

For a 25° slope

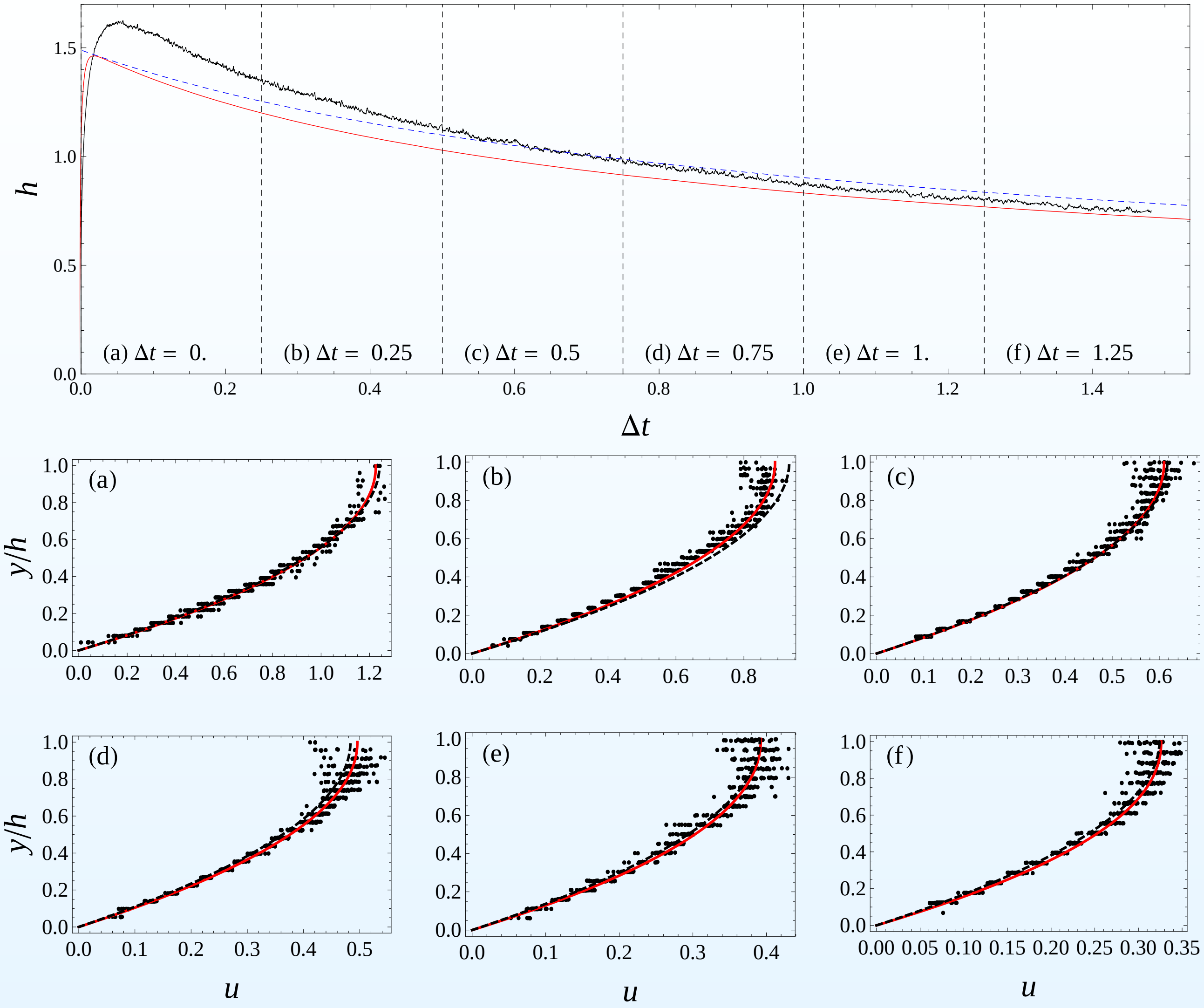

For a 25° slope, but $\phi = 0.45$

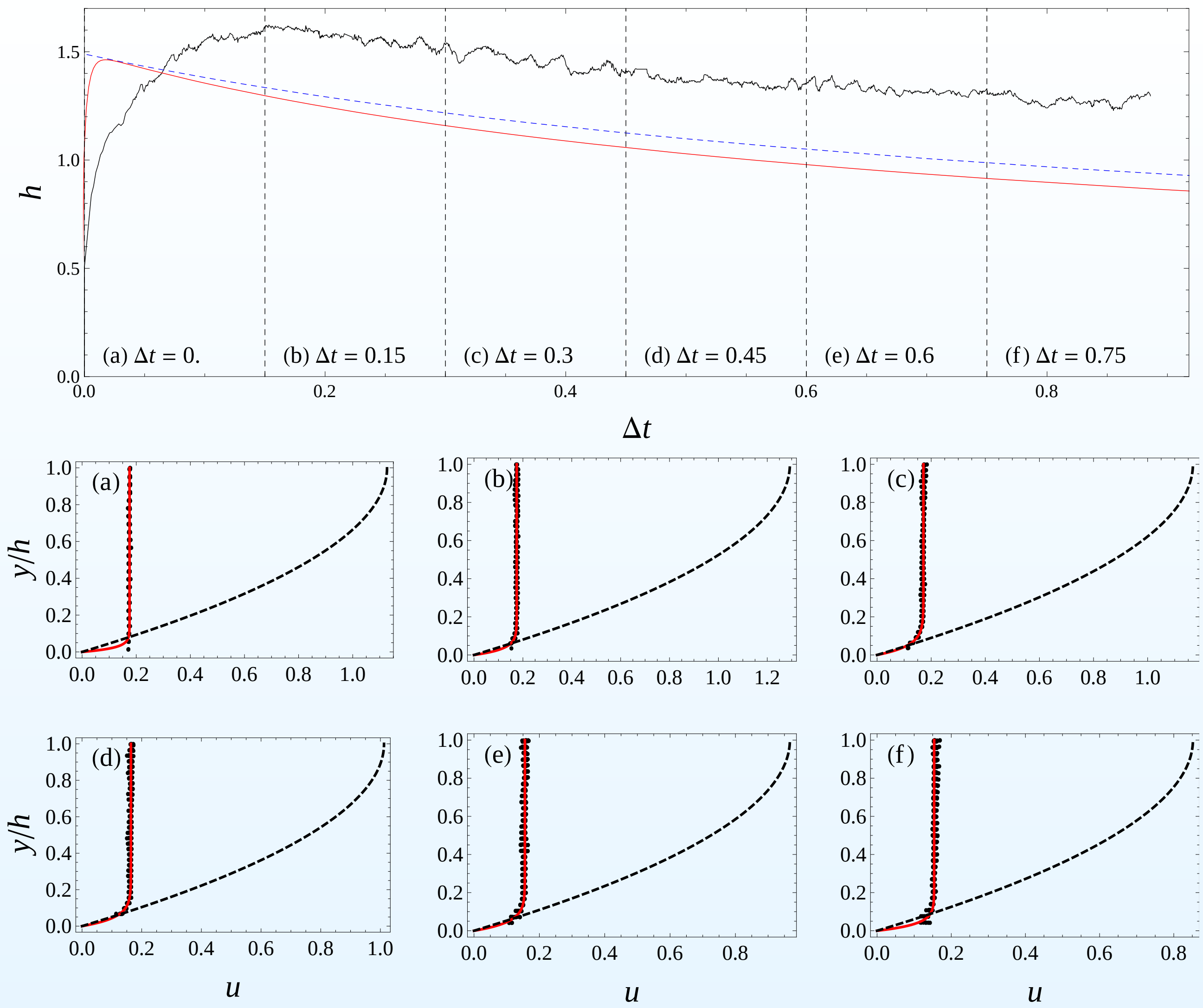

For a 25° slope, but $\phi = 0.57$

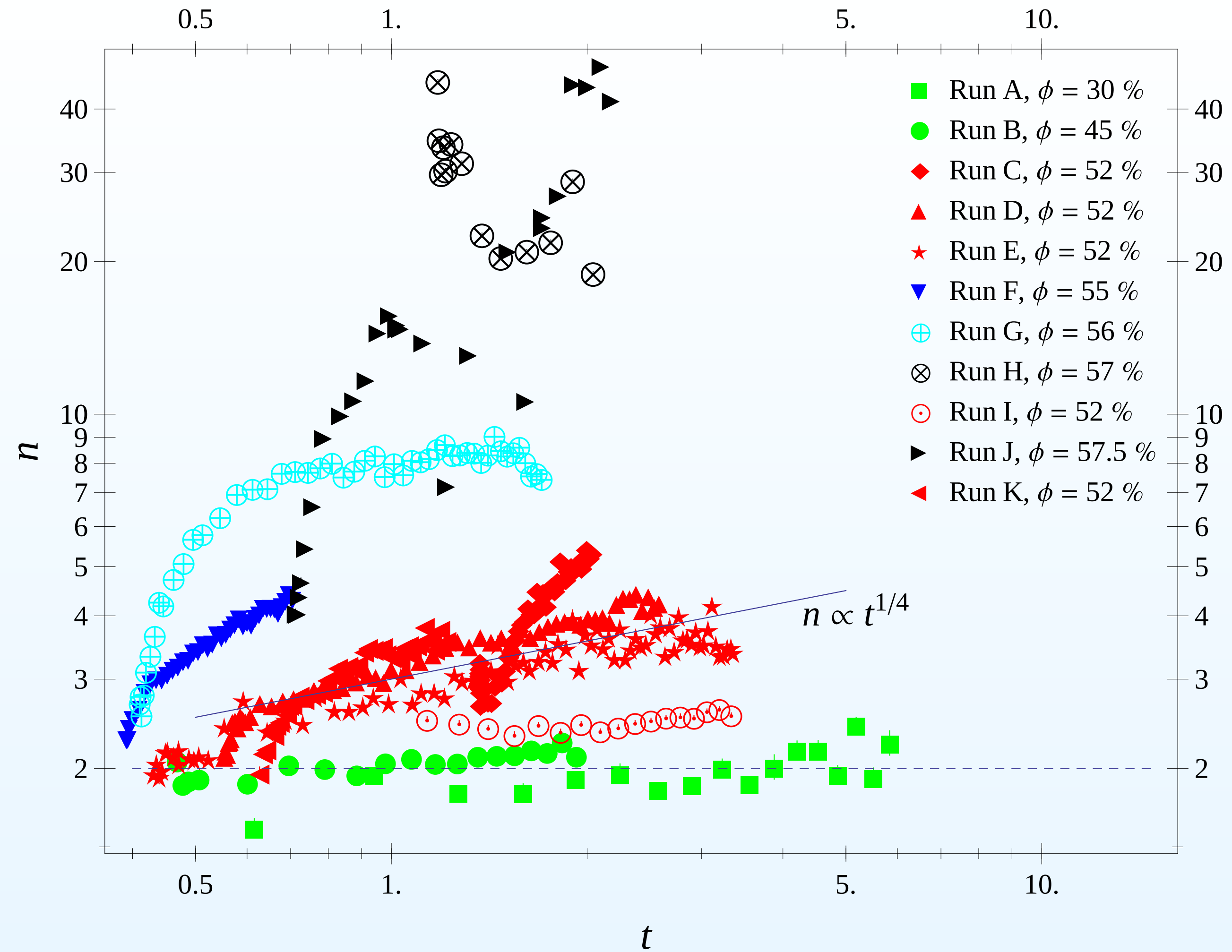

Variation of n with time (dimensionless)

ÉCOLE POLYTECHNIQUE
FÉDÉRALE DE LAUSANNE

Behaviour at the highest concentrations

For $\phi > 0.575$, behaviour is complicated, with three phases observed:

- *macro-viscous regime* at short times: $x_f \propto t^{1/3}$, parabolic profile of u,
- *fracture regime*: wavy free surface, fracture, and *en-masse* flow,
- *plastic regime*: intermittent motion (stick-slip).

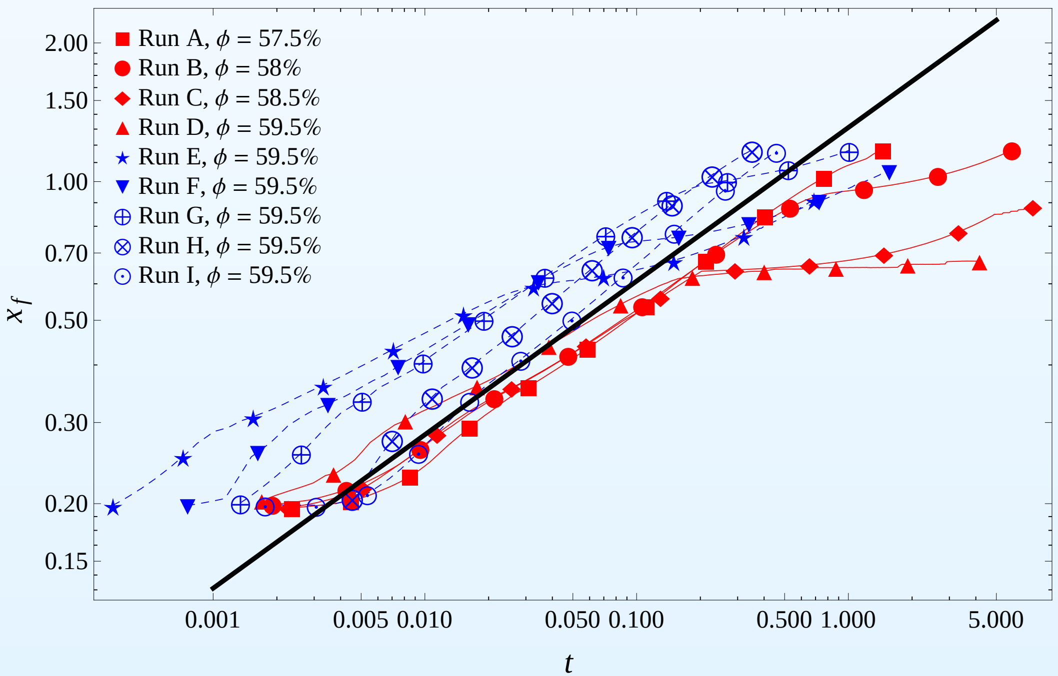

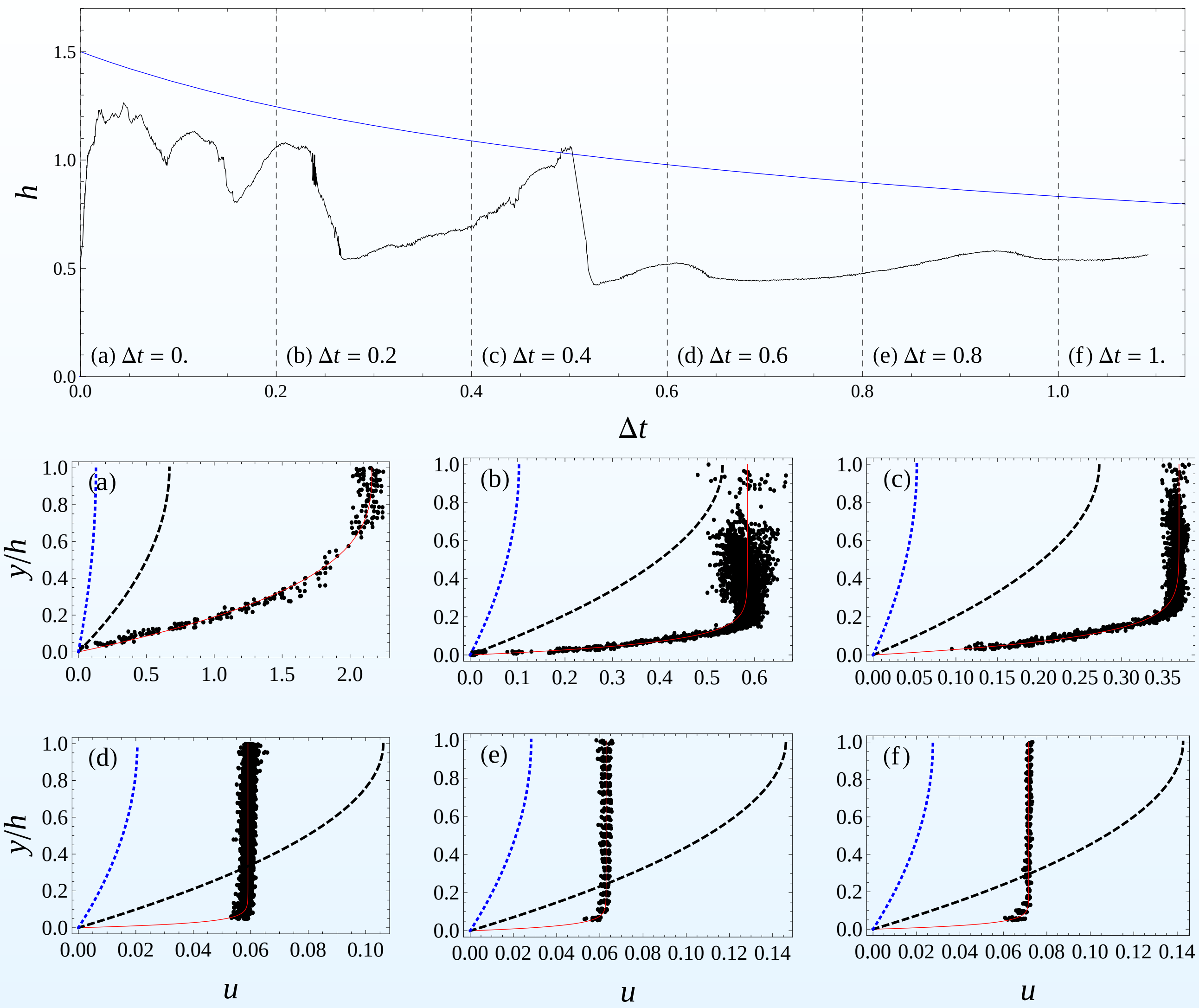

For 25° slope, $\phi = 0.595$

Stick-slip regime

Variation of the flow depth and the pressure 'head' $h_p = p/(\varrho g \cos\theta)$

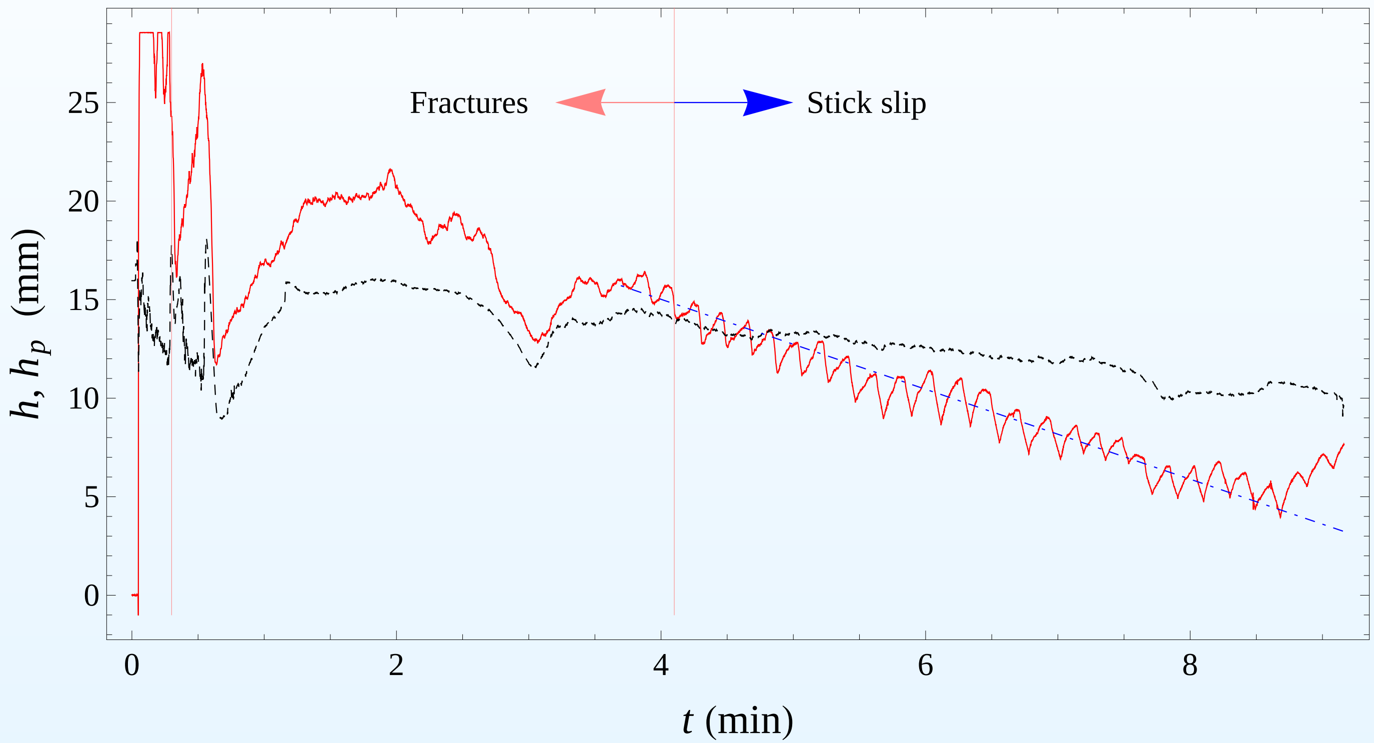

Experiments

$$\phi = 0.56$$

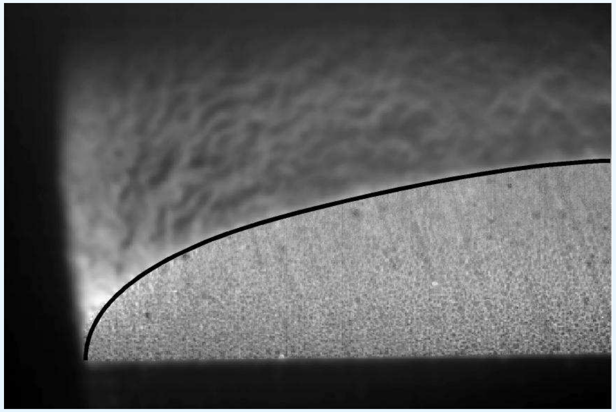

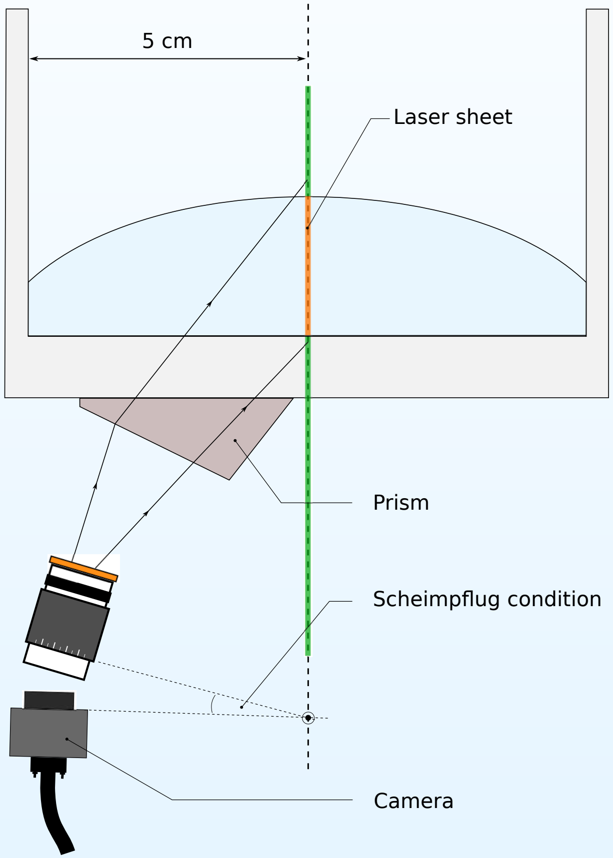

$$\phi = 0.595$$

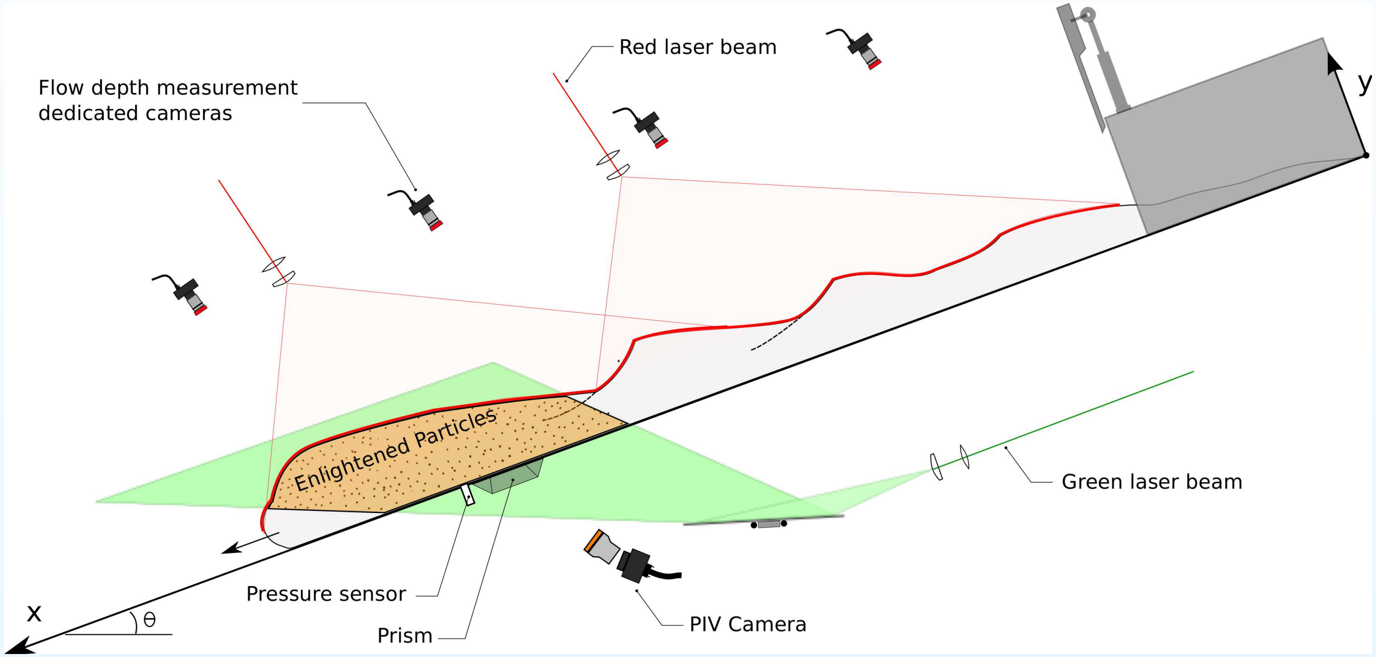
Red laser beam
Flow depth measurement
dedicated cameras
y
Enlightened Particles
Green laser beam
Pressure sensor
Prism
PIV Camera
x
θ

Conclusions

The dam-break for different rheologies. Our main findings:

- For Newtonian fluids: fairly good agreement between theory/experiment.
- For viscoplastic fluids: the simplest models perform better than more elaborate models such as Saint-Venant.
- For granular suspensions: we observed *macro-viscous* behaviour for concentrations as high as $\phi = 0.57$, then for higher concentrations, complicated behaviour, including stick-slip motion (resulting from a pore-pressure diffusion mechanism that is still poorly understood).

References

- Ancey, C., S. Cochard, and N. Andreini, The dam-break problem for viscous fluids in the high-capillary-number limit, JFM, 624, 1-22, 2009.
- Ancey, C., and S. Cochard, The dam-break problem for Herschel-Bulkley fluids down steep flumes, JNNFM, 158, 18-35, 2009.
- Andreini, N., Epely-Chauvin, and C. Ancey, Internal dynamics of Newtonian and viscoplastic fluid avalanches down a sloping bed, PoF, 24, 053101, 2012.
- Ancey, C., N. Andreini, and Epely-Chauvin, Viscoplastic dam break waves: review of simple computational approaches and comparison with experiments, Adv. Water Res., 48, 79-91, 2012.
- Ancey, C., N. Andreini, and Epely-Chauvin, The dam-break problem for concentrated suspensions of neutrally buoyant particles, JFM, 724, 95-122, 2013.
- Ancey, C., N. Andreini, and Epely-Chauvin, Granular suspensions I. Macro-viscous behavior, PoF, 25, 033301, 2013.
- Andreini, N., C. Ancey, and Epely-Chauvin, Granular suspensions. II. Plastic regime, PoF, 25, 033302, 2013.